

# Hyperspectral imaging applied to chalk reservoirs in the North Sea

The hyperspectral imaging method calibrated  
to the chalk mineralogy of the  
Ekofisk Formation  
in the SIF-1X well

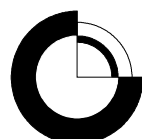
Morten L. Hjuler, Niels Hemmingsen Schovsbo,  
Rikke Weibel & Finn Jakobsen

# Hyperspectral imaging applied to chalk reservoirs in the North Sea

## The hyperspectral imaging method calibrated to the chalk mineralogy of the Ekofisk Formation in the SIF-1X well

Morten L. Hjuler, Niels Hemmingsen Schovsbo,  
Rikke Weibel & Finn Jakobsen

Released 01.05.2021



## **Indhold**

<b>1.</b>	<b>Executive summary</b>	<b>4</b>
<b>2.</b>	<b>Introduction</b>	<b>5</b>
<b>3.</b>	<b>The SIF-1X well</b>	<b>6</b>
<b>4.</b>	<b>Methods</b>	<b>8</b>
4.1	Hyperspectral imaging .....	8
4.2	Handheld X-ray fluorescence (HH-XRF) .....	8
4.3	Ultraviolet (UV) core photos.....	9
4.4	Principal component analysis (PCA) .....	9
<b>5.</b>	<b>Results</b>	<b>11</b>
5.1	Mineralogy based on hyperspectral imaging .....	11
5.2	Mineralogy based on HH-XRF .....	11
5.3	UV core photos .....	11
5.4	Principal component analysis (PCA) .....	11
<b>6.</b>	<b>Discussion</b>	<b>20</b>
<b>7.</b>	<b>Conclusions</b>	<b>21</b>
<b>8.</b>	<b>Recommendations</b>	<b>22</b>
<b>9.</b>	<b>References</b>	<b>23</b>

## **1. Executive summary**

Hyperspectral imaging provides fast mineralogical characterisation of core material from heterogeneous reservoirs and is a valuable and cost efficient first characterisation method that is already a commercial service provided to the industry.

In this study, we compare data obtained from hyperspectral imaging with high quality core photos (daylight and UV) and high resolution HH XRF data. The study clearly confirms that reliable rock typing can be made by hyperspectral recording even without performing additional chalk specific calibration of the rock libraries applied in the interpretation. For advanced rock typing, the hyperspectral data are, however, subordinate to what can be gained from core studies and (visual) image interpretation.

The cost reduction potential of hyperspectral imaging is thus well documented, as it will allow a first rock characterisation to be made in a systematic manner and in large volumes that will amount to compete core storage inventory. Based on hyperspectral imaging and complemented with existing data, specialists will obtain a high degree of information of reservoir heterogeneities and a solid base for selecting the best sampling sites. In order to provide a more detailed characterisation, the hyperspectra rock library needs to be updated with the specific rock types present in the targeted reservoirs such as clean chalk, marly chalk etc. in order to constitute a sufficiently accurate mineralogy characterisation tool.

Hyperspectral measurements were performed on slabbed core surfaces from cores of the SIF-1X well representing the lowermost 25 m of the Ekofisk Formation. In order to calibrate the spectra to fit the actual rock characteristics, spectral measurements were selected from four core intervals and compared with data from Handheld XRF (HH-XRF) analysis performed on the same core intervals. HH-XRF analysis provided a fast overview of mineralogical composition of the slabbed core surface and provides the reference data for calibration of spectra. Core photos obtained in ultraviolet (UV) light can be used to perform rough assessments of oil saturation and indirectly indicate silica and clay content.

## **2. Introduction**

Hyperspectral imaging provides fast mineralogical characterisation of core material from heterogeneous reservoirs and is a valuable fast and cost efficient first characterisation that is already a commercial service provided to the industry.

Hyperspectral Imaging of rock surfaces within the visible near-infrared and the short-wave infrared spectra can be used to map mineralogical and textural difference at high resolution and is applicable to a wide range of geological materials in settings ranging from mining to reservoir characterisation.

This study investigates the usage of hyperspectral imaging for enhanced chalk reservoir characterisation. Focus has been to develop a method to resolve the spatial distribution of silica and clay but also on detecting textural variation of the chalk matrix. The investigation includes existing, recently collated spectral imaging data and will aim at establishing and improving the rock type calibration and thus ensure full interpretation of data.

Future perspectives include full imaging of the core archive and mapping of mineralogical and textural properties. For the latter, we recommend that the hyperspectral imaging method is calibrated to the rock types of North Sea chalk. Further, the method allows fast characterisation of core material from heterogeneous reservoirs and identification of silicified sections with possible impact on porosity, permeability and geomechanical properties.

### 3. The SIF-1X well

The SIF-1X well is located in the Halfdan Field in the southern part of the Danish Central Graben in the North Sea (Figure 1). SIF-1X was drilled in 1999 as an exploration well focussing on reservoir quality, stratigraphy and hydrocarbon content of chalcs of the Maastrichtian Tor Formation and the Danian Ekofisk Formation (Mærsk Olie og Gas A/S 2000). Top chalk (Ekofisk Fm) was encountered at 2012 m TVDSS and TD at 2193 m TVDSS (Tor Fm). Six cores totalling 68 m and with a recovery percentage of 98.16% were cut in the Tor and Ekofisk formations (Table 1).

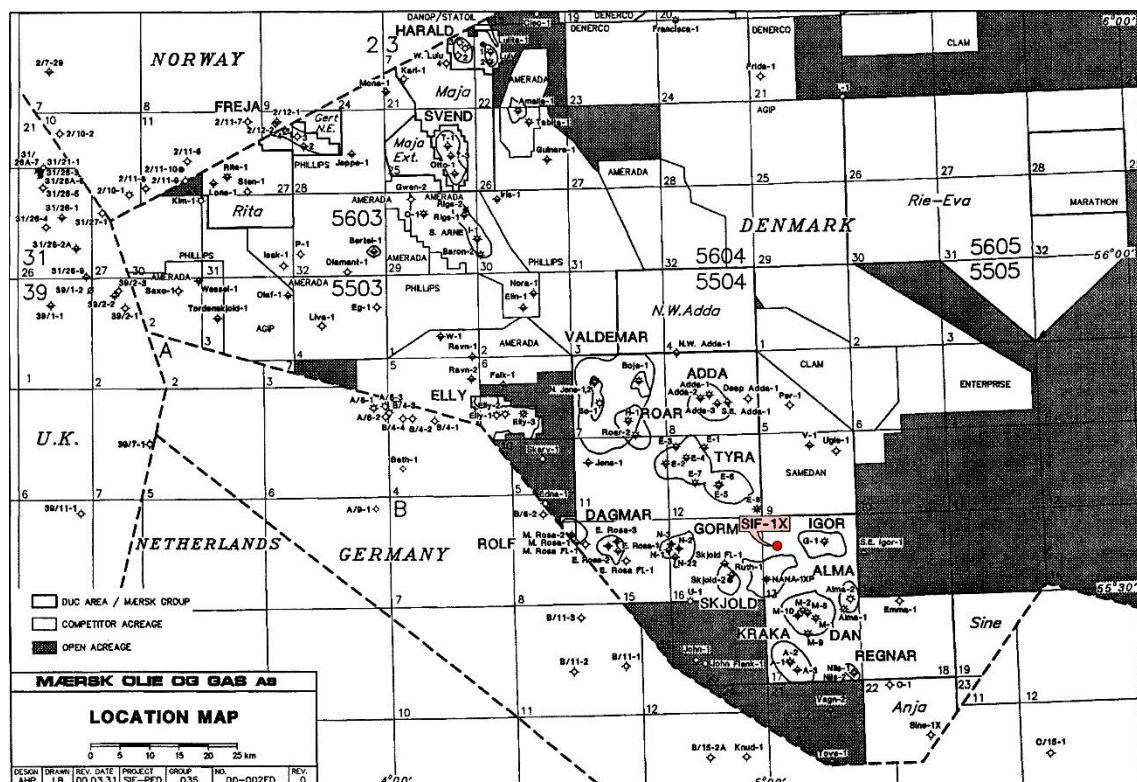


**Figure 1. Location of the SIF-1X well in the southern part of the Danish Central Graben in the North Sea. Modified from Mærsk Olie og Gas A/S (2000).**

**Table 1. Overview of cored intervals in the Ekofisk and Tor formations in the SIF-1X well. Shaded cores (2–4) have been partly or completely subjected to hyperspectral imaging.**

Core	Box	Recovery	Formation	Age	Depth interval (m TVDSS)
1		0%	Ekofisk	Danian	2011–2013
2	1–22	95%	Ekofisk	Danian	2013–2031
3	1–22	100%	Ekofisk	Danian	2031–2049
4	1–5	100%	Ekofisk	Danian	2049–2053
5		0%	Tor	Maastrichtian	2053–2053
6	1–33	100%	Tor	Maastrichtian	2059–2087

The lithological variation from pure chalk intervals to partly or completely silicified intervals as well as the presence of stylolites and clay-rich intervals makes the Ekofisk Formation a sensible choice in terms of studying how well hyperspectral imaging differentiates between various lithologies.

## 4. Methods

In order to calibrate the hyperspectral spectra obtained from the SIF-1X well to fit the actual rock characteristics, the obtained spectra was compared with chemical data from handheld X-ray fluorescence (HH-XRF) analysis performed on slabbed core samples selected from intervals subjected to hyperspectral imaging. In addition,

Further, a minor feasibility study was conducted by applying multilinear regressive models to the relationship between the calibrated spectral response and existing core data such as porosity, permeability, rock strength and chemical data obtained from HH-XRF analysis. This study tested the possibility of making predictive functional rock typing based on spectral data.

Four core intervals were selected for this study comprising:

- Core 2, box 21            2029.47–2030.36 m (TVDSS)
- Core 3, box 1            2030.89–2031.50 m (TVDSS)
- Core 3, box 10          2038.84–2039.75 m (TVDSS)
- Core 4, box 1            2050.30–2051.21 m (TVDSS)

### 4.1 Hyperspectral imaging

The hyperspectral imaging method generates 2D images where each pixel contains information from hundreds of spectral channels in the *near visible–shortwave infrared spectrum* (NV–SWIR) (0.9–1.7 mm) and the *longwave infrared spectrum* (LWIR) (8–14 mm). These spectra are invisible to the human eye and capable of storing far more information than regular cameras with three visible RGB colour channels (400–700 nm). Hyperspectral imaging is applied in material identification and process detection.

### 4.2 Handheld X-ray fluorescence (HH-XRF)

Measuring was done using a handheld NitonTM XI3t Goldd+ XRF device (HH-XRF) at the core storage of Mærsk Oil & Gas, Baltikavej, Copenhagen, Denmark. The device is equipped with an Ag anode that measures at 6–50 kV and up to 200 µA and provides semi-quantitative element concentrations. Measuring area is about 5mm in diameter. The HH-XRF instrument was mounted on a specially constructed test table allowing full contact between the slabbed cores and probing device.

Measuring time was 2 minutes per measuring point, applying the “test all geo filter” that measured dually on low and high filters. Measurements were performed directly on the slabbed core surface. Measurements of both in-house and certified powder samples were made to ensure data quality and reliability (c.f. Schovsbo et al. 2018).

Measuring points were mainly selected based on visible mineralogy, i.e. silicified intervals, clay-enriched intervals as wells as intervals of pure calcite in order to secure registration of mineralogy variations of the core slabs. In order to validate the measurements, the slab surface were subjected to measurements in both sides, which for convenience are referred to as the left and right side. The measuring points are shown in Fig. 2.

### 4.3 Ultraviolet (UV) core photos

Ultraviolet imaging illustrates oil saturation. A bright yellow response corresponds to high saturation, dark colour to no saturation. Oil saturation indirectly indicates silica and clay content. Further, UV core photos were used to generate a relative oil saturation curve with 5 steps, step 1 representing 0% oil saturation and step 5 assumed to represent 100 % or nearly 100% oil saturation.

### 4.4 Principal component analysis (PCA)

PCA performed on HH-XRF data was used for defining rock types for calibration of the hyperspectral rock model. Only reliable determined elements were used for PCA rock-typing. Lg2-normalization opens the data to better deal with forced correlations. Outliers were removed. For method description see Esbensen (2012).

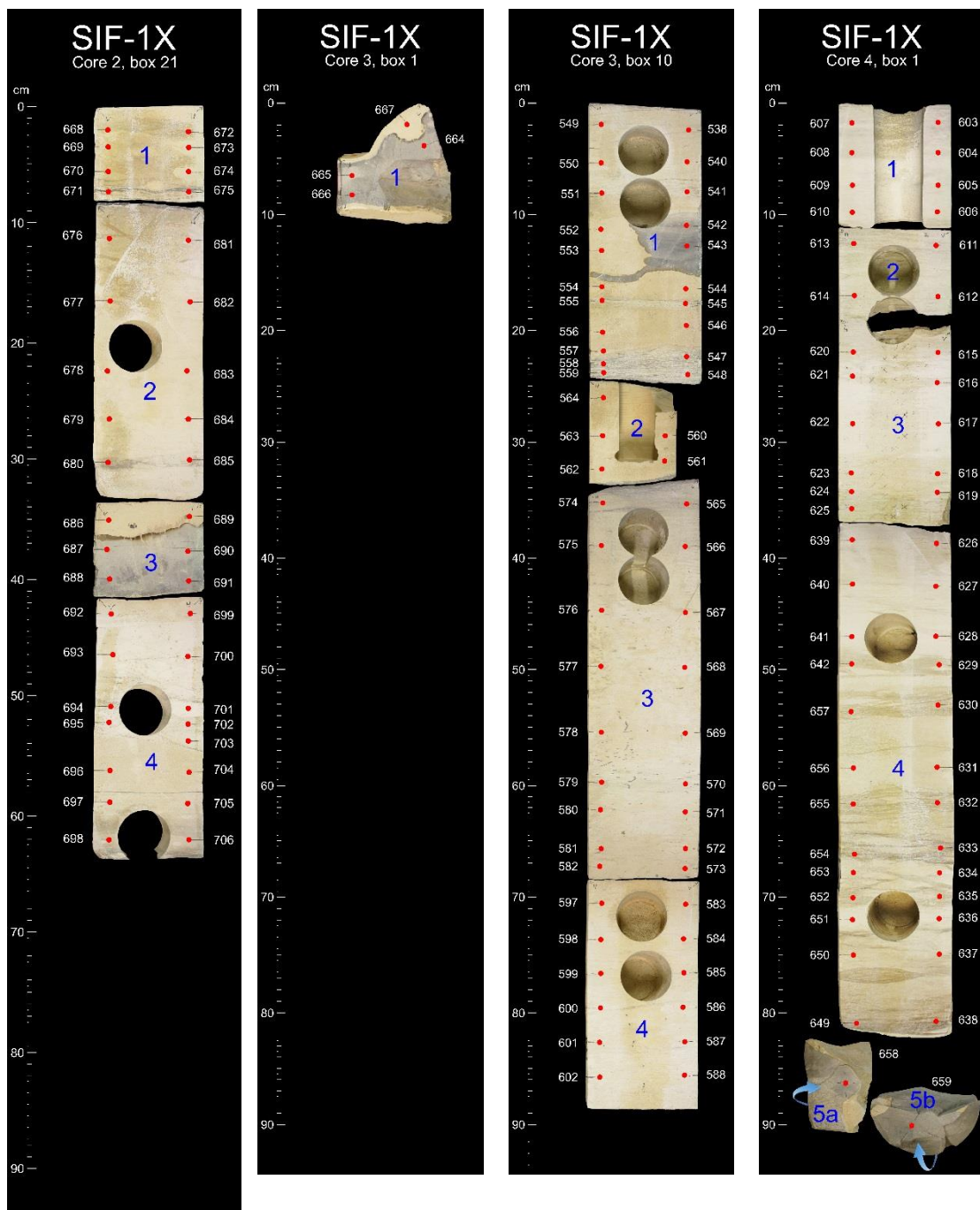


Figure 2. HH-XRF-analysed slabs. Measuring points (red dots) and numbers are shown. Blue numbers indicate core piece.

## 5. Results

### 5.1 Mineralogy based on hyperspectral imaging

The hyperspectral mineralogy identification is presented in Figs 3–6. Generally, calcite (chalk) is identified satisfactorily when compared with core photos and HH-XRF results; however, clay-enriched sections, which are clearly visible on core photos, may not be identified. Strongly silicified sections, which are visibly determined as flint, are identified as either opal, quartz, fine-grained quartz, fine-grained quartz-clay or Al-smectite, the latter obviously, being incorrect. The LWIR and SWIR spectra generally produce similar mineralogy maps for the core slabs; however, in silicified sections the type of silica identified vary between the spectra. Further, the amount and type of clay observed in calcite-dominated intervals may vary between the LWIR and SWIR spectra.

### 5.2 Mineralogy based on HH-XRF

The mineralogy inferred from HH-XRF data satisfactorily describes the distribution of calcite (chalk), flint and silica-rich sections, whereas identification of clay species is more challenging due to the low concentrations of elements such as Al, K and Fe.

One important result obtained of the HH\_XRF analysis is a frequently observed inconsistency between measurements from the left and right sides of the core slab. Significantly elevated Chlorine (Cl) concentrations were measured on the right side of the slab (Figs 7–8).

Mineralogy

### 5.3 UV core photos

The oil saturation variations revealed by UV core photos proved a useful support for the mineralogy interpretations obtained by hyperspectral imaging and HH-XRF. Reservoir sections saturated with oil correspond with high calcite content. In contrast flint bands show no saturation and clay-rich sections show various degrees of clay saturation.

As a further result, the UV photos allow the generation of a relative oil saturation curve (Fig. 9).

### 5.4 Principal component analysis (PCA)

The results of the PCA model of HH-XRF is shown in Figs 10–11. First two PC components display the main structure of the data.

Five rock types have been identified:

- Chalk with low salt content
- Chalk with high salt content
- Nearly pure silica (flint)
- Chalk with similar amounts of carbonate and silica
- Chalk with high clay content

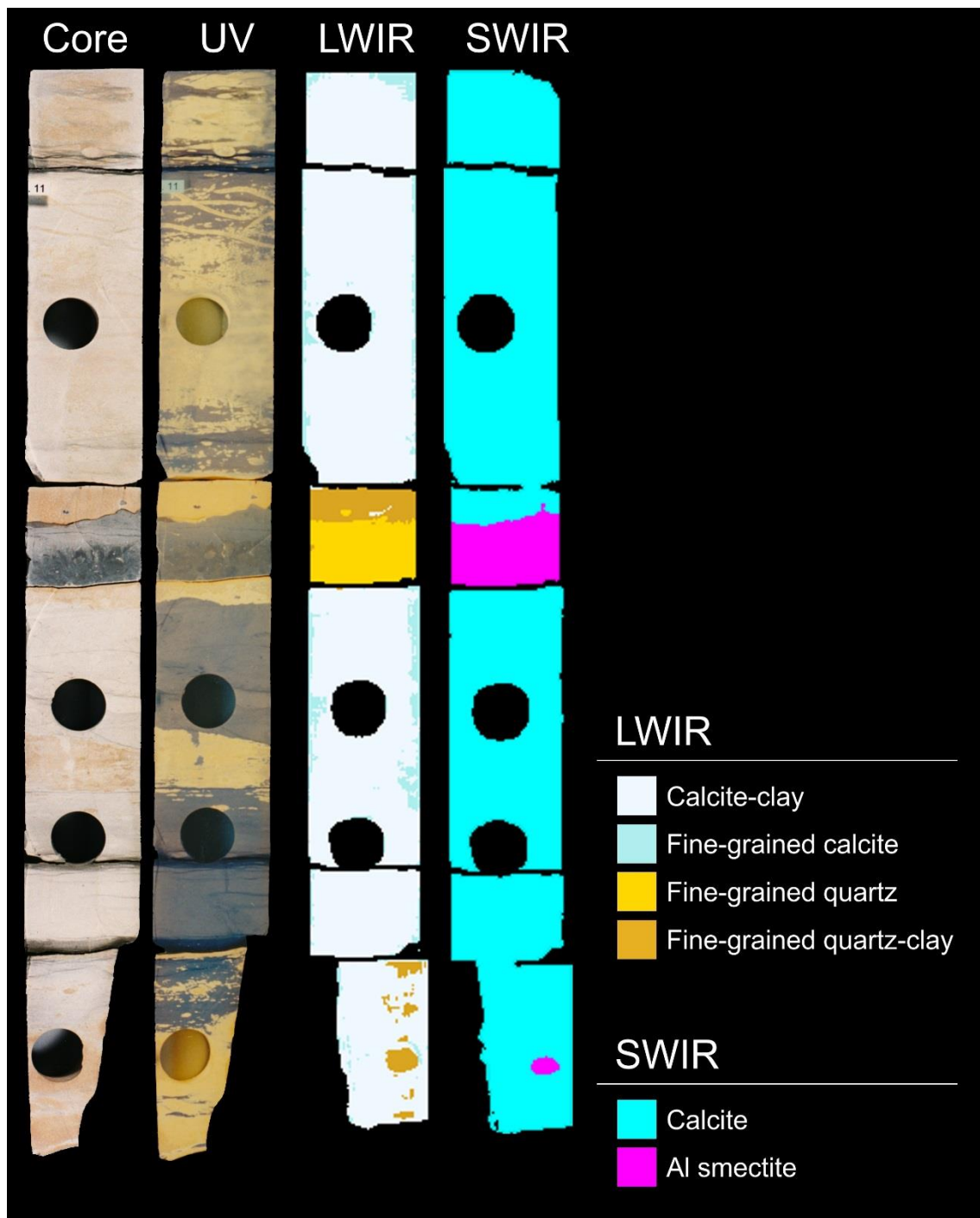


Figure 3. Mineralogy results from LWIR and SWIR spectra compared with core photos and ultraviolet (UV) photos. Note that SWIR spectra identify the flint band in the core middle as Al smectite. SIF-1X, core 2, box 21.

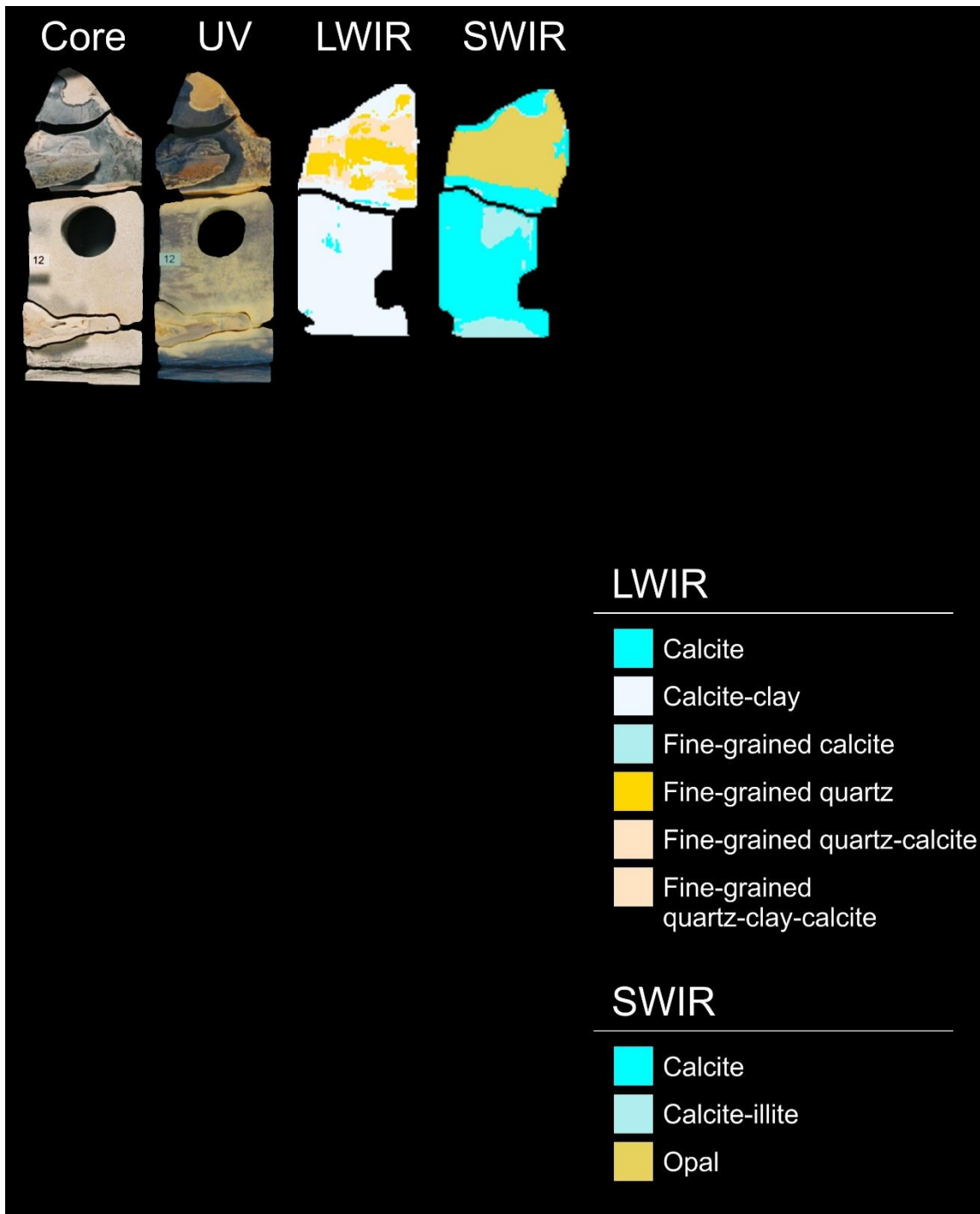


Figure 4. Mineralogy results from LWIR and SWIR spectra compared with core photos and ultraviolet (UV) photos. Note variations between LWIR and SWIR spectra regarding the flint band at the core top. SIF-1X, core 3, box 1.

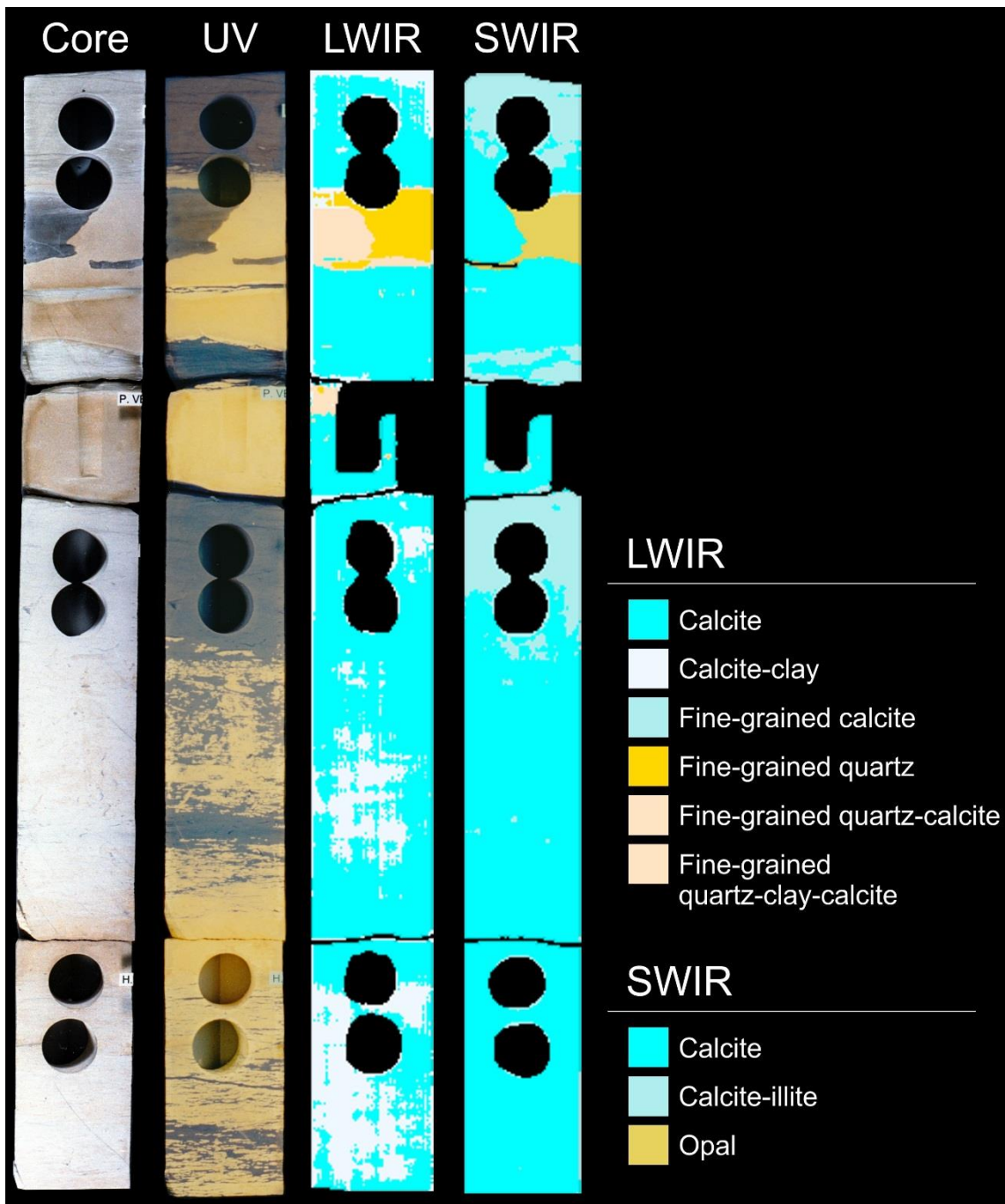


Figure 5. Mineralogy results from LWIR and SWIR spectra compared with core photos and ultraviolet (UV) photos. SIF-1X, core 3, box 10.

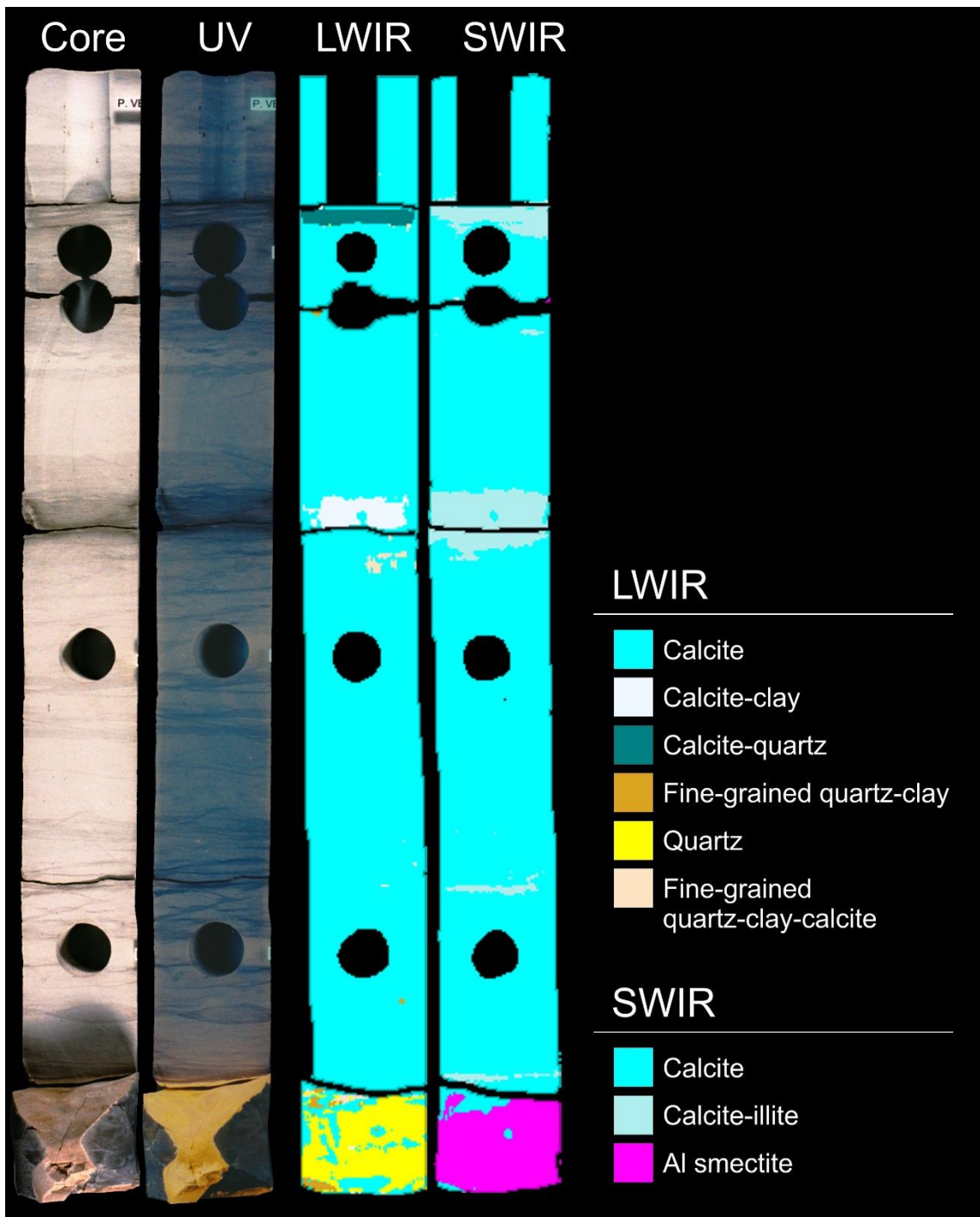


Figure 6. Mineralogy results from LWIR and SWIR spectra compared with core photos and ultraviolet (UV) photos. Note variations between LWIR and SWIR spectra regarding the flint band at the core base. SIF-1X, core 4, box 2.

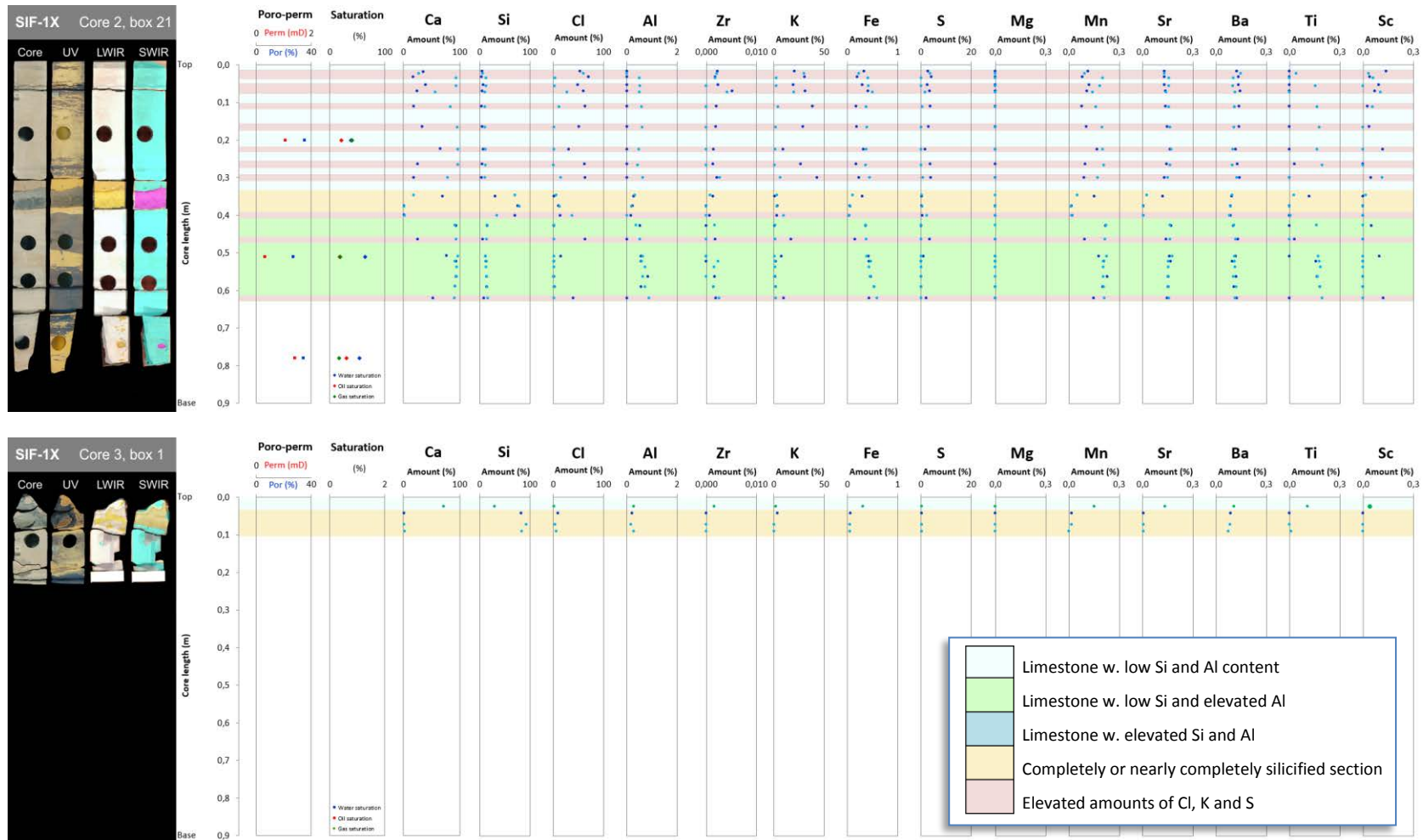


Figure 7. Mineralogy of the core slabs of core 2, box 21 and core 3, box 1 determined from the HH-XRF analysis. The mineralogy is compared with core photos, ultraviolet (UV) photos and LWIR and SWIR spectra.

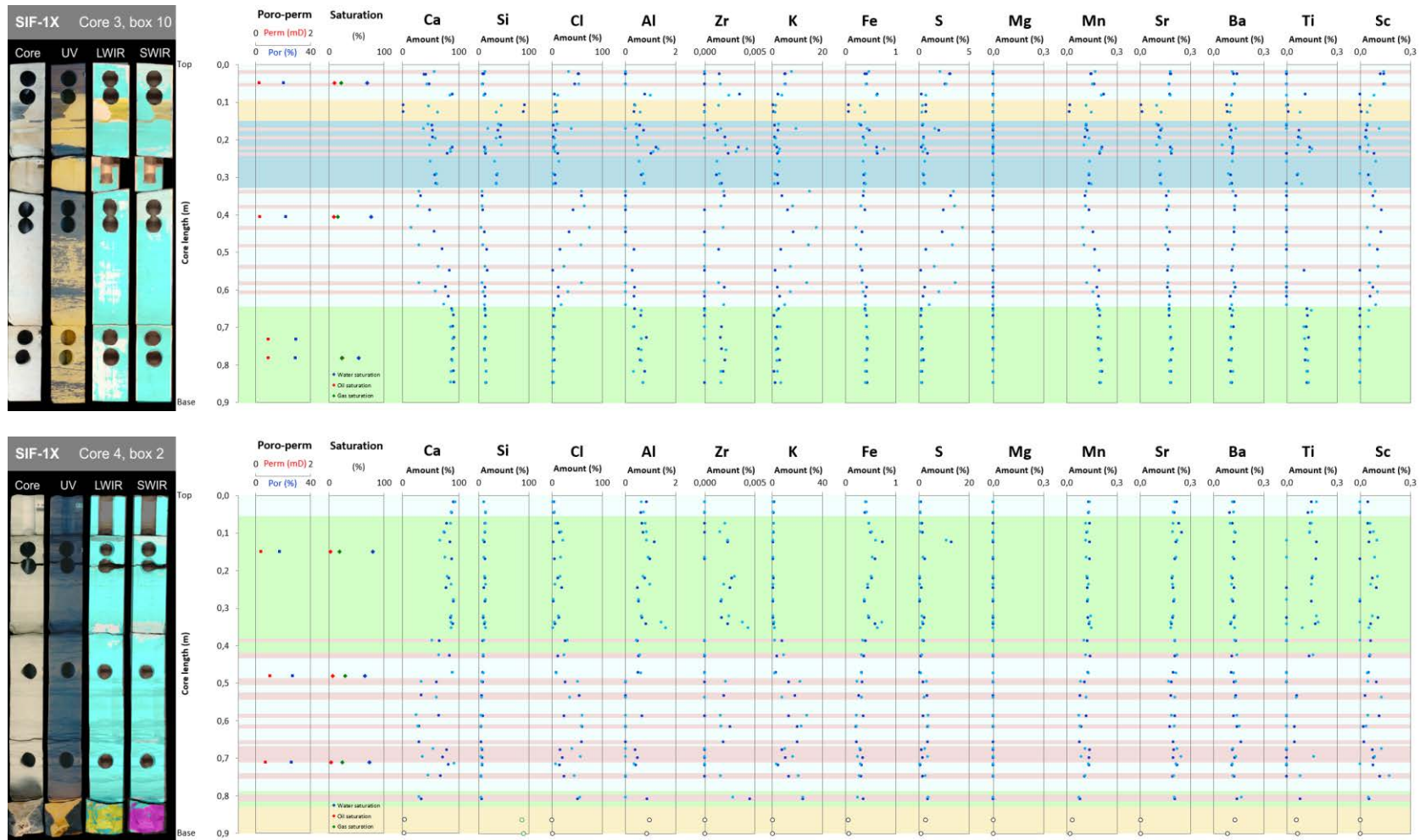


Figure 8. Mineralogy of the core slabs of core 3, box 10 and core 4, box 2 determined from the HH-XRF analysis. The mineralogy is compared with core photos, ultraviolet (UV) photos and LWIR and SWIR spectra. For mineralogical legend, refer to Fig. 7.

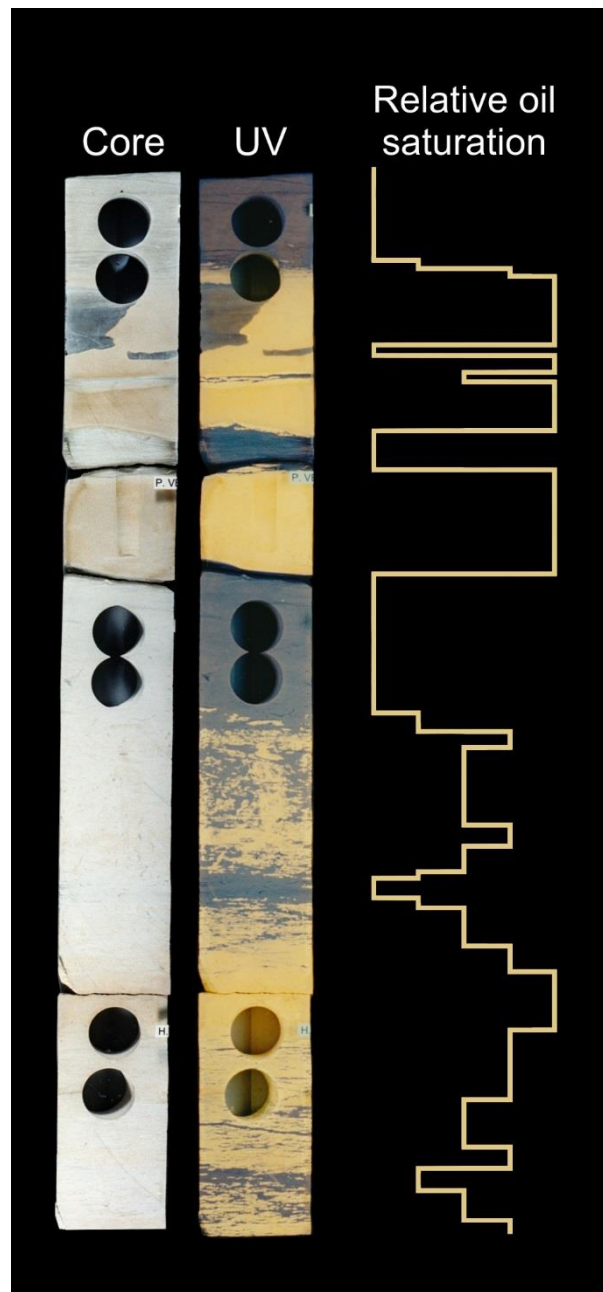


Figure 9. Relative oil saturation curve generated from ultraviolet (UV) photos. SIF-1X, core 3, box 10.

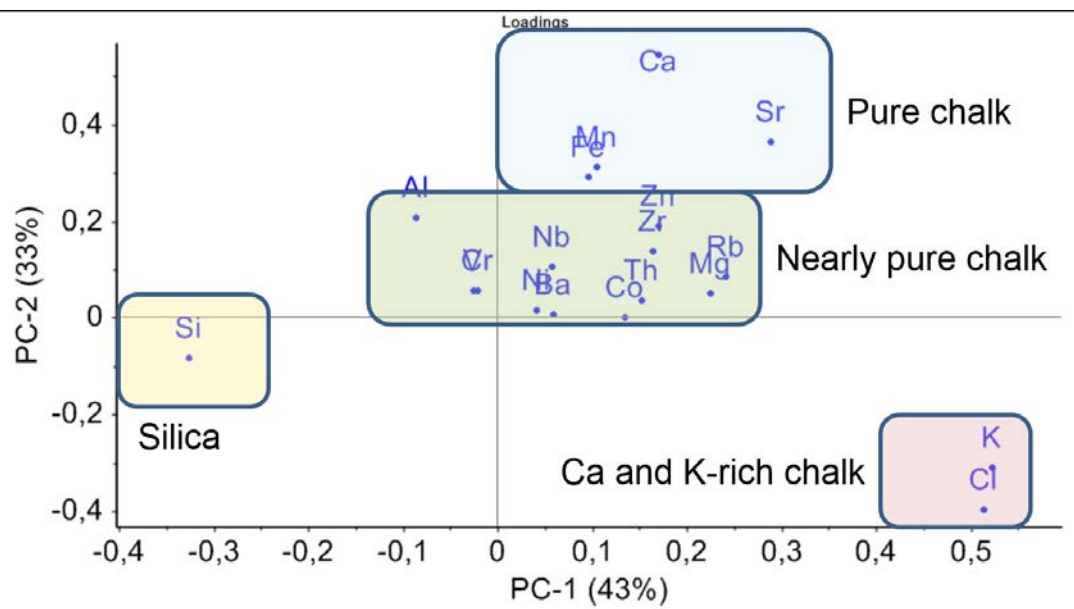


Figure 10. Loading plot, principal component axis 1 (PC-1) versus principal component (PC) axis 2 (PC-1).

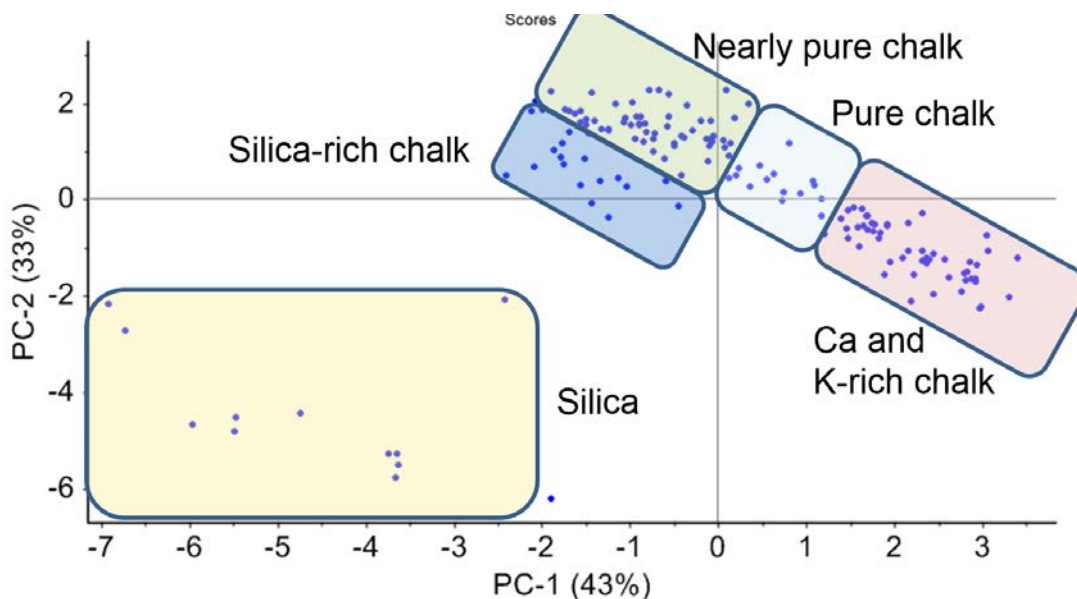


Figure 11. Score plot, principal component axis 1 (PC-1) versus principal component (PC) axis 2 (PC-1).

## 6. Discussion

Hyperspectral imaging in its present uncalibrated state does not fulfil its purpose satisfactorily due to uncertainties regarding mainly the calcite–clay relation and the silica–clay relation. Sections of elevated clay content were observed in core and UV photos but not in the hyperspectra. With respect to measuring clay elements, the HH-XRF method may hint at their presence, but the measuring uncertainty is high due to low count numbers. Further, the high content of Cl, which is interpreted as a source of error, obscures the true relation between measured elements and thus minerals.

The sporadic but frequent, high content of Cl obtained by the HH-XRF method is explained either as halite precipitated from formation water at the surface or in pores near the surface, or as an infiltration constituent from bore mud. In the final well report, bore mud discharge is specified as containing a significant amount of KCl and as peaks of Cl content coincide with corresponding peaks of K, bore mud infiltration constitutes a reliable explanation. Still, a theory explaining why the Cl content is significantly higher than the Ca content in several measurements is lacking.

The variation between Cl values across the core may be indicative of core orientation during storage. Low values are invariably located to one side of the core and high values to the opposite side of the core. This variation may be explained by core orientation during storage and implies that gravity forces pore water to the lower side of the core where suspended ions precipitate as the pore water evaporates.

## 7. Conclusions

Hyperspectral imaging has the potential to provide fast and possibly reliable characterisation of chalk cores; however, the hyperspectra used in this study show uncertainties frequent uncertainties, especially in relation to clay. A calibration of the hyperspectral data is necessary, before the potential is unlocked.

Some general trends were observed during the study:

Regarding oil saturation:

- UV core photos allow generation of a relative oil saturation curve
- High salt content (K and Cl) is found in water-saturated, oil-free, porous chalk
- Low salt content is found in oil-saturated porous chalk
- The current hyperspectral index does not allow identification
- of oil saturation in chalk
- Cl and K may originate from evaporating pore water

Regarding silicification

- *Silicified zones*: General agreement between HI and HH-XRF

Regarding chalk

- *Pure chalk*: No clear relation between HI and HH-XRF
- *Clay-rich zones*: some agreement between HI and HH-XRF
- *Cl and K-rich zones*: only detected by HH-XRF
- *Cl and K-rich zones*: possible agreement between HH-XRF and UV core photos

## **8. Recommendations**

Calibration of the hyperspectra are needed in order for hyperspectral imaging to constitute a reliable tool for providing fast characterisation of core material from heterogeneous reservoirs. X-ray diffraction (XRD), scanning electron microscopy and detailed core description may provide additional calibration data and should be considered.

## 9. References

**Esbensen, K.H. 2012:** Multivariate data analysis, in practise: an introduction to multivariate data analysis and experimental design 598 pp. CAMO publishing, Oslo, Norway.

**Mærsk Olie og Gas A/S 2000:** Final well report. Volume 1(2): Well Sif-1X, Sif-1XA, Sif-1XB, Sif-1XC, Sif-1XD. 269 p.

**Schovsbo, N.H., Nielsen A.T., Harstad, A.O., Bruton, D.L., 2018:** Stratigraphy and geochemical composition of the Cambrian Alum Shale Formation in the Porsgrunn core, Skien-Langesund district, southern Norway. Bulletin of the Geological Society of Denmark 66, 1–20.

	Well					Measuring points					hh-XRF Measurements (normalized)														
Reading No	Well	Core	Box	Core Piece	Depth m	Distance between top box and top of core piece mm	Distance between top box and measuring point m	Depth m	Location on well core slab	Visual Lithology	Ca %	Si %	Cl %	K %	Al %	Mg %	S %	Fe %	Mn %	Sr %	Ba %	Ti %	Sc %	Zr %	
538	SIF-1X	3	10	1	2074,24	7	0,026	2074,27	Left	Chalk	38,207	10,050	53,773	4,995	0,000	0,000	3,129	0,392	0,144	0,184	0,142	0,000	0,119	0,000	
539	SIF-1X	3	10	1	2074,24	7	0,026	2074,27	Left	Chalk	40,923	8,366	52,496	5,353	0,000	3,362	3,081	0,418	0,147	0,182	0,119	0,000	0,141	0,001	
540	SIF-1X	3	10	1	2074,24	7	0,053	2074,29	Left	Chalk	47,825	8,678	45,553	5,331	0,000	0,000	2,588	0,421	0,164	0,174	0,128	0,000	0,141	0,000	
541	SIF-1X	3	10	1	2074,24	7	0,080	2074,32	Left	Clay and chalk	89,007	13,098	4,844	2,370	0,779	0,000	0,264	0,634	0,220	0,179	0,114	0,112	0,000	0,004	
542	SIF-1X	3	10	1	2074,24	7	0,109	2074,35	Left	flint	0,915	92,214	6,632	0,353	0,369	0,000	0,678	0,063	0,020	0,006	0,079	0,006	0,000	0,000	
543	SIF-1X	3	10	1	2074,24	7	0,127	2074,37	Left	flint	1,096	90,136	8,962	0,417	0,350	0,000	0,694	0,059	0,015	0,011	0,084	0,007	0,004	0,000	
544	SIF-1X	3	10	1	2074,24	7	0,164	2074,40	Left	Chalk	52,713	43,896	2,988	0,877	0,568	0,000	0,373	0,310	0,116	0,110	0,097	0,000	0,041	0,000	
545	SIF-1X	3	10	1	2074,24	7	0,177	2074,42	Left	Clay and chalk	53,408	38,712	6,767	2,406	0,739	0,000	1,982	0,479	0,123	0,122	0,107	0,071	0,036	0,001	
546	SIF-1X	3	10	1	2074,24	7	0,196	2074,44	Left	Chalk	53,815	42,733	2,450	1,009	0,455	0,000	0,496	0,349	0,110	0,113	0,101	0,068	0,032	0,002	
547	SIF-1X	3	10	1	2074,24	7	0,223	2074,46	Left	Clay and chalk	88,892	11,529	3,414	1,845	1,231	0,000	0,248	0,624	0,211	0,180	0,116	0,138	0,000	0,003	
548	SIF-1X	3	10	1	2074,24	7	0,240	2074,48	Left	Clay and chalk	80,080	14,455	11,186	2,178	1,013	0,000	0,873	0,639	0,198	0,188	0,113	0,000	0,082	0,002	
549	SIF-1X	3	10	1	2074,24	0	0,019	2074,26	Right	Chalk	56,173	12,378	33,508	7,790	0,000	0,000	2,082	0,469	0,170	0,182	0,115	0,000	0,141	0,000	
550	SIF-1X	3	10	1	2074,24	0	0,053	2074,29	Right	Chalk	43,079	7,440	52,754	5,102	0,000	0,000	2,708	0,411	0,153	0,173	0,126	0,000	0,146	0,002	
551	SIF-1X	3	10	1	2074,24	0	0,083	2074,32	Right	Clay and chalk	84,340	10,611	11,894	3,876	0,994	0,000	0,708	0,627	0,207	0,180	0,110	0,000	0,083	0,002	
552	SIF-1X	3	10	1	2074,24	0	0,111	2074,35	Right	Chalk	46,823	45,897	7,532	1,502	0,399	0,000	0,373	0,297	0,116	0,100	0,105	0,000	0,059	0,001	
553	SIF-1X	3	10	1	2074,24	0	0,129	2074,37	Right	Chalk	62,656	35,708	3,277	1,255	0,600	0,000	0,280	0,384	0,148	0,126	0,101	0,080	0,041	0,000	
554	SIF-1X	3	10	1	2074,24	0	0,160	2074,40	Right	Chalk	45,385	40,092	10,345	2,493	0,425	0,000	0,402	0,275	0,116	0,101	0,099	0,000	0,044	0,001	
555	SIF-1X	3	10	1	2074,24	0	0,173	2074,41	Right	Clay and chalk	37,216	18,111	39,185	9,443	0,000	0,000	1,622	0,430	0,115	0,132	0,133	0,000	0,113	0,002	
556	SIF-1X	3	10	1	2074,24	0	0,199	2074,44	Right	Chalk	58,097	35,056	4,860	1,506	0,464	0,000	0,459	0,368	0,134	0,120	0,108	0,084	0,040	0,000	
557	SIF-1X	3	10	1	2074,24	0	0,217	2074,46	Right	Chalk	48,309	45,393	6,915	1,052	0,507	0,000	0,427	0,397	0,102	0,101	0,051	0,065	0,048	0,002	
558	SIF-1X	3	10	1	2074,24	0	0,227	2074,47	Right	Clay and chalk	85,391	13,828	4,135	3,088	1,313	0,000	0,647	0,768	0,208	0,192	0,117	0,149	0,000	0,004	
559	SIF-1X	3	10	1	2074,24	0	0,235	2074,48	Right	Clay and chalk	86,091	12,888	5,613	2,610	1,103	0,000	0,400	0,628	0,196	0,184	0,116	0,136	0,043	0,003	
560	SIF-1X	3	10	2	2074,24	276	0,297	2074,54	Left	Chalk	57,766	36,594	5,962	1,999	0,644	0,000	0,479	0,369	0,134	0,121	0,103	0,062	0,048	0,001	
561	SIF-1X	3	10	2	2074,24	276	0,320	2074,56	Left	Chalk	59,185	35,176	7,027	2,287	0,760	0,000	0,531	0,374	0,134	0,124	0,110	0,000	0,058	0,002	
564	SIF-1X	3	10	2	2074,24	245	0,260	2074,50	Right	Chalk	49,602	31,549	13,376	2,744	0,556	0,000	0,605	0,357	0,137	0,115	0,114	0,000	0,092	0,001	
563	SIF-1X	3	10	2	2074,24	245	0,294	2074,53	Right	Chalk	60,345	37,230	2,179	1,244	0,697	0,000	0,427	0,387	0,134	0,122	0,089	0,067	0,000	0,001	
562	SIF-1X	3	10	2	2074,24	245	0,322	2074,56	Right	Chalk	61,865	34,843	2,655	1,053	0,743	0,000	0,582	0,402	0,147	0,128	0,101	0,088	0,064	0,001	
565	SIF-1X	3	10	3	2074,24	330	0,353	2074,59	Left	Chalk	31,905	6,862	58,684	3,794	0,000	0,000	3,171	0,348	0,110</td						

600	SIF-1X	3	10	4	2074,24	685	0,797	2075,04	Right	Chalk	89,090	14,319	1,981	1,983	0,648	0,000	0,264	0,401	0,202	0,179	0,106	0,128	0,000	0,000
601	SIF-1X	3	10	4	2074,24	685	0,826	2075,07	Right	Chalk	86,699	14,621	2,384	2,168	0,325	0,000	0,201	0,399	0,201	0,179	0,118	0,119	0,000	0,002
602	SIF-1X	3	10	4	2074,24	685	0,856	2075,10	Right	Chalk	86,114	13,834	4,208	3,528	0,715	0,000	0,229	0,394	0,204	0,181	0,105	0,131	0,000	0,002
603	SIF-1X	4	1	1	2085,7	7	0,017	2085,72	Left	Chalk	90,509	11,094	4,004	1,691	0,838	0,000	0,723	0,408	0,132	0,218	0,124	0,147	0,047	0,000
604	SIF-1X	4	1	1	2085,7	7	0,046	2085,75	Left	Chalk	87,435	13,918	3,505	0,912	0,626	0,000	0,549	0,390	0,129	0,205	0,096	0,128	0,000	0,000
605	SIF-1X	4	1	1	2085,7	7	0,074	2085,77	Left	Clay and chalk	78,580	12,879	11,803	0,828	0,656	0,000	1,265	0,462	0,135	0,232	0,113	0,139	0,047	0,000
606	SIF-1X	4	1	1	2085,7	7	0,098	2085,80	Left	Clay and chalk	74,799	12,279	15,262	0,839	0,711	0,000	1,394	0,499	0,121	0,249	0,129	0,138	0,061	0,000
607	SIF-1X	4	1	1	2085,7	0	0,017	2085,72	Right	Chalk	93,689	10,801	1,384	0,590	0,636	0,000	0,404	0,395	0,137	0,208	0,114	0,179	0,000	0,000
608	SIF-1X	4	1	1	2085,7	0	0,045	2085,75	Right	Chalk	86,905	14,236	4,977	0,560	0,723	0,000	0,512	0,423	0,135	0,199	0,120	0,152	0,000	0,000
609	SIF-1X	4	1	1	2085,7	0	0,074	2085,77	Right	Clay and chalk	85,366	13,825	6,747	0,978	0,805	1,719	0,493	0,468	0,113	0,197	0,100	0,146	0,058	0,002
610	SIF-1X	4	1	1	2085,7	0	0,097	2085,80	Right	Clay and chalk	73,261	12,940	18,358	0,893	0,846	0,000	0,560	0,520	0,122	0,193	0,126	0,136	0,078	0,002
611	SIF-1X	4	1	2	2085,7	111	0,124	2085,82	Left	Clay and chalk	84,388	11,753	2,405	0,764	1,150	0,000	12,955	0,735	0,137	0,214	0,125	0,178	0,052	0,002
612	SIF-1X	4	1	2	2085,7	111	0,169	2085,87	Left	Chalk	87,960	12,546	4,595	0,620	0,979	0,000	2,248	0,590	0,138	0,209	0,125	0,174	0,000	0,000
613	SIF-1X	4	1	2	2085,7	106	0,119	2085,82	Right	Clay and chalk	66,548	9,490	21,740	0,493	0,842	0,000	10,843	0,596	0,115	0,220	0,328	0,000	0,101	0,002
614	SIF-1X	4	1	2	2085,7	106	0,164	2085,86	Right	Chalk	75,768	11,034	17,121	0,441	0,900	0,000	1,614	0,531	0,117	0,214	0,116	0,000	0,088	0,000
615	SIF-1X	4	1	3	2085,7	202	0,220	2085,92	Left	ler+krift	82,272	12,643	11,733	1,034	0,772	0,000	0,377	0,523	0,125	0,191	0,114	0,150	0,074	0,003
616	SIF-1X	4	1	3	2085,7	202	0,246	2085,95	Left	ler+krift	77,429	10,116	19,274	0,503	0,479	0,000	1,033	0,442	0,125	0,199	0,123	0,000	0,095	0,003
617	SIF-1X	4	1	3	2085,7	202	0,282	2085,98	Left	Chalk	90,703	13,361	2,686	0,686	0,515	0,000	0,234	0,373	0,125	0,203	0,116	0,147	0,000	0,002
618	SIF-1X	4	1	3	2085,7	202	0,325	2086,03	Left	Chalk	85,225	9,105	14,270	0,502	0,661	0,000	2,012	0,462	0,126	0,194	0,123	0,000	0,105	0,002
619	SIF-1X	4	1	3	2085,7	202	0,342	2086,04	Left	Clay and chalk	89,195	11,597	6,322	1,060	0,827	0,000	1,624	0,584	0,133	0,187	0,103	0,171	0,062	0,002
620	SIF-1X	4	1	3	2085,7	187	0,216	2085,92	Right	Clay and chalk	80,032	11,515	15,632	0,693	0,694	0,000	0,384	0,513	0,120	0,195	0,106	0,000	0,103	0,003
621	SIF-1X	4	1	3	2085,7	187	0,237	2085,94	Right	Clay and chalk	86,322	14,224	5,804	0,591	0,966	0,000	0,220	0,440	0,131	0,196	0,110	0,153	0,064	0,002
622	SIF-1X	4	1	3	2085,7	187	0,278	2085,98	Right	Chalk	90,507	13,516	3,009	0,388	0,529	0,000	0,271	0,378	0,127	0,203	0,108	0,147	0,000	0,002
623	SIF-1X	4	1	3	2085,7	187	0,321	2086,02	Right	Chalk	86,855	9,764	12,478	0,493	0,646	0,000	1,203	0,450	0,144	0,197	0,126	0,000	0,071	0,002
624	SIF-1X	4	1	3	2085,7	187	0,338	2086,04	Right	Clay and chalk	86,763	12,777	4,768	1,436	1,433	0,000	1,316	0,723	0,136	0,185	0,107	0,176	0,000	0,004
625	SIF-1X	4	1	3	2085,7	187	0,353	2086,05	Right	Clay and chalk	86,629	13,398	1,705	1,843	1,603	0,000	0,630	0,146	0,183	0,128	0,188	0,052	0,004	0,004
626	SIF-1X	4	2	4	2085,7	377	0,387	2086,09	Left	Clay and chalk	65,624	7,955	26,258	7,822	0,473	0,000	1,770	0,399	0,123	0,207	0,135	0,000	0,064	0,000
627	SIF-1X	4	2	4	2085,7	377	0,427	2086,13	Left	Clay and chalk	84,115	9,535	11,139	3,587	0,533	0,000	0,660	0,365	0,142	0,210	0,110	0,134	0,056	0,000
628	SIF-1X	4	2	4	2085,7	377	0,471	2086,17	Left	Chalk	88,174	8,843	7,685	2,671	0,508	1,816	0,336	0,314	0,128	0,197	0,108	0,000	0,048	0,000
629	SIF-1X	4	2	4	2085,7	377	0,497	2086,20	Left	Clay and chalk	60,922	8,353	26,154	13,182	0,000	0,000	1,607	0,328	0,108	0,188	0,125	0,000	0,098	0,000
630	SIF-1X	4	2	4	2085,7	377	0,532	2086,23	Left	Clay and chalk	33,467	5,748	53,880	18,209	0,000	0,000	3,332	0,266	0,080	0,185	0,134	0,061	0,029	0,002
631	SIF																							

668	SIF-1X	2	21	1	2064,87	0	0,018	2064,89	Left	Chalk	35,653	4,985	53,914	20,399	0,000	0,000	2,879	0,326	0,113	0,131	0,125	0,000	0,137	0,002
669	SIF-1X	2	21	1	2064,87	0	0,033	2064,90	Left	Chalk	17,218	3,717	69,961	30,907	0,000	0,000	4,204	0,196	0,079	0,131	0,134	0,000	0,039	0,002
670	SIF-1X	2	21	1	2064,87	0	0,054	2064,92	Left	Chalk	39,106	6,818	48,301	19,636	0,000	0,000	2,609	0,297	0,119	0,132	0,132	0,000	0,093	0,002
671	SIF-1X	2	21	1	2064,87	0	0,070	2064,94	Left	Clay and chalk	23,908	5,060	60,177	31,328	0,000	0,000	3,389	0,411	0,106	0,137	0,143	0,000	0,070	0,005
672	SIF-1X	2	21	1	2064,87	0	0,023	2064,89	Right	Chalk	27,199	5,810	59,584	29,805	0,000	0,000	3,625	0,233	0,094	0,130	0,148	0,041	0,034	0,002
673	SIF-1X	2	21	1	2064,87	0	0,035	2064,91	Right	Chalk	94,193	12,320	3,570	2,645	0,507	0,000	0,152	0,412	0,202	0,156	0,103	0,000	0,059	0,002
674	SIF-1X	2	21	1	2064,87	0	0,056	2064,93	Right	Chalk	93,402	12,463	2,429	2,215	0,529	0,000	0,110	0,421	0,185	0,157	0,101	0,153	0,000	0,000
675	SIF-1X	2	21	1	2064,87	0	0,073	2064,94	Right	Clay and chalk	56,894	10,454	27,587	20,034	0,499	0,000	1,567	0,504	0,142	0,139	0,114	0,000	0,103	0,004
676	SIF-1X	2	21	2	2064,87	79	0,110	2064,98	Left	Chalk	18,360	3,336	63,888	38,293	0,000	0,000	3,680	0,175	0,078	0,137	0,138	0,000	0,024	0,002
677	SIF-1X	2	21	2	2064,87	79	0,164	2065,03	Left	Chalk	33,283	4,872	51,507	28,994	0,000	0,000	2,947	0,189	0,105	0,147	0,138	0,000	0,037	0,002
678	SIF-1X	2	21	2	2064,87	79	0,224	2065,09	Left	Chalk	65,289	7,081	30,888	9,496	0,000	0,000	1,631	0,318	0,167	0,165	0,117	0,000	0,117	0,001
679	SIF-1X	2	21	2	2064,87	79	0,264	2065,13	Left	Chalk	25,560	4,959	62,031	26,526	0,000	0,000	3,756	0,177	0,095	0,144	0,127	0,028	0,000	0,001
680	SIF-1X	2	21	2	2064,87	79	0,300	2065,17	Left	Chalk	18,407	3,348	63,265	43,206	0,000	0,000	3,904	0,229	0,091	0,131	0,141	0,000	0,046	0,002
681	SIF-1X	2	21	2	2064,87	82	0,112	2064,98	Right	Chalk	84,137	10,857	11,186	4,201	0,590	0,000	0,625	0,378	0,162	0,159	0,111	0,163	0,056	0,000
682	SIF-1X	2	21	2	2064,87	82	0,166	2065,04	Right	Chalk	95,434	11,161	1,645	2,046	0,618	0,000	0,107	0,393	0,200	0,164	0,107	0,178	0,000	0,000
683	SIF-1X	2	21	2	2064,87	82	0,225	2065,10	Right	Chalk	96,514	11,263	1,375	1,129	0,486	0,000	0,119	0,373	0,203	0,171	0,101	0,166	0,000	0,000
684	SIF-1X	2	21	2	2064,87	82	0,266	2065,14	Right	Chalk	96,680	11,748	0,722	0,536	0,427	2,203	0,088	0,367	0,208	0,166	0,097	0,193	0,000	0,000
685	SIF-1X	2	21	2	2064,87	82	0,300	2065,17	Right	Chalk	78,561	11,147	15,337	6,249	0,631	0,000	0,842	0,447	0,171	0,150	0,123	0,000	0,112	0,003
686	SIF-1X	2	21	3	2064,87	335	0,350	2065,22	Left	Chalk	69,330	31,019	1,892	1,041	0,282	1,184	0,210	0,300	0,151	0,121	0,092	0,116	0,000	0,001
687	SIF-1X	2	21	3	2064,87	335	0,375	2065,25	Left	Flint	1,213	76,097	10,616	3,393	0,228	0,000	0,403	0,050	0,016	0,006	0,086	0,000	0,000	0,000
688	SIF-1X	2	21	3	2064,87	335	0,400	2065,27	Left	Flint	0,849	70,392	13,423	2,995	0,156	0,000	0,513	0,040	0,018	0,005	0,088	0,000	0,000	0,001
689	SIF-1X	2	21	3	2064,87	335	0,346	2065,22	Right	Chalk	18,205	70,751	5,942	2,857	0,325	0,000	0,296	0,107	0,049	0,027	0,098	0,026	0,017	0,001
690	SIF-1X	2	21	3	2064,87	335	0,376	2065,25	Right	Flint	1,296	79,520	13,220	3,052	0,195	0,000	0,608	0,064	0,013	0,005	0,087	0,000	0,000	0,000
691	SIF-1X	2	21	3	2064,87	335	0,401	2065,27	Right	Flint	1,672	34,573	37,720	9,531	0,000	0,000	2,320	0,039	0,015	0,005	0,080	0,006	0,000	0,000
692	SIF-1X	2	21	4	2064,87	415	0,428	2065,30	Left	Chalk	94,229	14,591	1,636	0,580	0,527	1,773	0,086	0,365	0,218	0,172	0,103	0,000	0,050	0,000
693	SIF-1X	2	21	4	2064,87	415	0,464	2065,33	Left	Chalk	25,200	5,884	63,850	16,958	0,000	0,000	3,474	0,149	0,092	0,140	0,130	0,029	0,000	0,002
694	SIF-1X	2	21	4	2064,87	415	0,508	2065,38	Left	Chalk	76,410	12,108	14,757	7,736	0,560	0,000	0,926	0,424	0,177	0,162	0,116	0,000	0,097	0,000
695	SIF-1X	2	21	4	2064,87	415	0,522	2065,39	Left	Chalk	93,619	13,092	1,853	1,668	0,579	0,000	0,080	0,431	0,210	0,169	0,095	0,158	0,000	0,000
696	SIF-1X	2	21	4	2064,87	415	0,563	2065,43	Left	Chalk	93,728	14,334	1,392	1,283	0,839	2,194	0,121	0,462	0,228	0,153	0,122	0,164	0,000	0,002
697	SIF-1X	2	21	4	2064,87	415	0,589	2065,46	Left	Chalk	91,258	14,128	2,325	1,995	0,569	0,000	0,076	0,530	0,202	0,155	0,108	0,182	0,000	0,001
698	SIF-1X	2	21	4	2064,87	415	0,620	2065,49	Left	Chalk	52,065	8,596	40,127	9,913	0,000	0,000	2,068	0,436	0,146	0,148	0,123	0,000	0,122	0,0

Well							Conventional core analysis						Dean Stark				
Sample ID	Well	Formation	Core	Box	Depth m MDRT	Depth Ft MDRT	Depth from core top m	Plug orientation	Plug diameter m	Plug length m	Porosity %	Air perm.	Klink. Perm. md	Density g/cm3	Water saturation %	Oil saturation %	Gas saturation %
51	SIF-1X	Ekofisk	2	21	2065,07	6775,2	0,20	hor			35,06	1,06	0,44	2,71	38,79	20,51	40,7
52	SIF-1X	Ekofisk	2	21	2065,38	6776,2	0,51	hor			26,87	0,308	0,1	2,7	64,3	17,33	18,37
53	SIF-1X	Ekofisk	2	21	2065,65	6777,1	0,78	hor			34,41	1,4	0,66	2,68	53,47	29,9	16,64
79	SIF-1X	Ekofisk	3	10	2074,29	6805,4	0,05	hor			20,15	0,135		2,71	68,97	8,98	22,05
80	SIF-1X	Ekofisk	3	10	2074,65	6806,6	0,41	hor			21,92	0,15		2,71	76,65	8,17	15,19
10X	SIF-1X	Ekofisk	3	10	2074,98	6807,7	0,74	hor			29,13	0,454	0,18	2,7			
81	SIF-1X	Ekofisk	3	10	2075,03	6807,8	0,79	hor			28,82	0,458	0,19	2,7	53,93	23,68	22,39
111	SIF-1X	Ekofisk	4	2	2085,85	6843,3	0,15	hor			17,43	0,186	-999	2,71	79,32	2,41	18,27
112	SIF-1X	Ekofisk	4	2	2086,18	6844,4	0,48	hor			26,87	0,517	0,22	2,7	64,57	6,24	29,2
113	SIF-1X	Ekofisk	4	2	2086,41	6845,2	0,71	hor			26,15	0,354	0,14	2,71	73,15	3,36	23,49

